TECHNICAL NOTE

# Interpretation of fringes obtained with coherent gradient sensing

Hareesh V. Tippur

An interference analysis for double-grating shearing interferometry called coherent gradient sensing is presented, and the results are compared with an earlier geometrical optics analysis and a Fourier optics analysis based on the Fresnel approximation. The influence of the order of approximation in these analyses and the equivalence of fringe interpretation in each case are discussed.

Lateral shearing interferometers that use a pair of Ronchi rulings for wave-front shearing have been widely used for many years for real-time testing of optical components.[1] However, experimental mechanics investigations using this interferometer, particularly experimental fracture mechanics studies, are a relatively recent development. A real-time lateral shearing interferometry with an on-line spatial filtering configuration called coherent gradient sensing (CGS) has been developed for quasi-static and dynamic fracture mechanics studies.[2–6] CGS is shown to measure in-plane gradients of hydrostatic stress when used in the transmission mode with optically isotropic transparent objects and in-plane gradients of out-of-plane displacement when used in the reflection mode with specularly reflective objects. A first-order analysis using geometrical optics[2] and a Fourier optics analysis using Fresnel diffraction[4] have indicated that full-field interference patterns obtained with CGS represent contours of the direction cosines of the local propagation vector, which can be further related to stress or a deformation field through a plane stress approximation. The objectives behind this Note are (1) to present a simple interference analysis and (2), more important, to demonstrate the equivalence of the analyses presented in Refs. 2 and 4, although a small difference in the two results is apparent owing to the order of approximation used in each case.

The author is with the Department of Mechanical Engineering, Auburn University, Auburn, Alabama 36849.

Received 12 October 1993; revised manuscript received 18 February 1994.

0003-6935/94/194167-04$06.00/0.



The optical arrangement for transmission CGS is shown in Fig. 1. It consists of a collimated beam of light propagating parallel to the optical axis. The beam is transmitted through a transparent specimen in the region of interest. The object wave front is diffracted as it propagates through Ronchi rulings (pitch $p$, grating lines parallel to, say, the $x$ axis) $G_1$ and $G_2$. Note that the two grating planes are separated by a distance $\Delta$ along the optical axis. It is reasonable to assume a square-wave transmission profile for the gratings, and hence the resulting diffracted wave fronts consist of a zeroth-order diffraction and several odd diffraction orders. [Chromium on glass master gratings with antireflection coatings with $p = 25$ μm and $\Delta = 30$–$100$ mm (Refs. 2–6) have produced satisfactory results.] For simplicity of representation, consider diffraction orders $E_0$, $E_{+1}$, and $E_{-1}$ only. Here $\theta$ is the diffraction angle [$\theta = \sin^{-1}(\lambda/p) \approx (\lambda/p)$]. The discrete wave fronts emerging from the grating $G_2$ are collected by the filtering lens, and the spectral contents are displayed on the back focal plane of the lens. A filtering aperture blocks all but $-1$ (or $+1$) diffraction orders as shown. The filtered information produces laterally sheared object wave fronts on the image plane. Note that the optical arrangement is such that the camera consisting of the filtering lens and the camera back is focused on the object plane.

Now consider the interference produced in the overlapping region of the two laterally sheared wave fronts on the image plane when the specimen (say, a uniform planar phase object) is undeformed [Fig. 2(a)]. Then interference is due to the path difference between $E_0$ and $E_{-1}$ as shown. The total complex amplitude on the image plane is $(E_0 + E_{-1})$. The

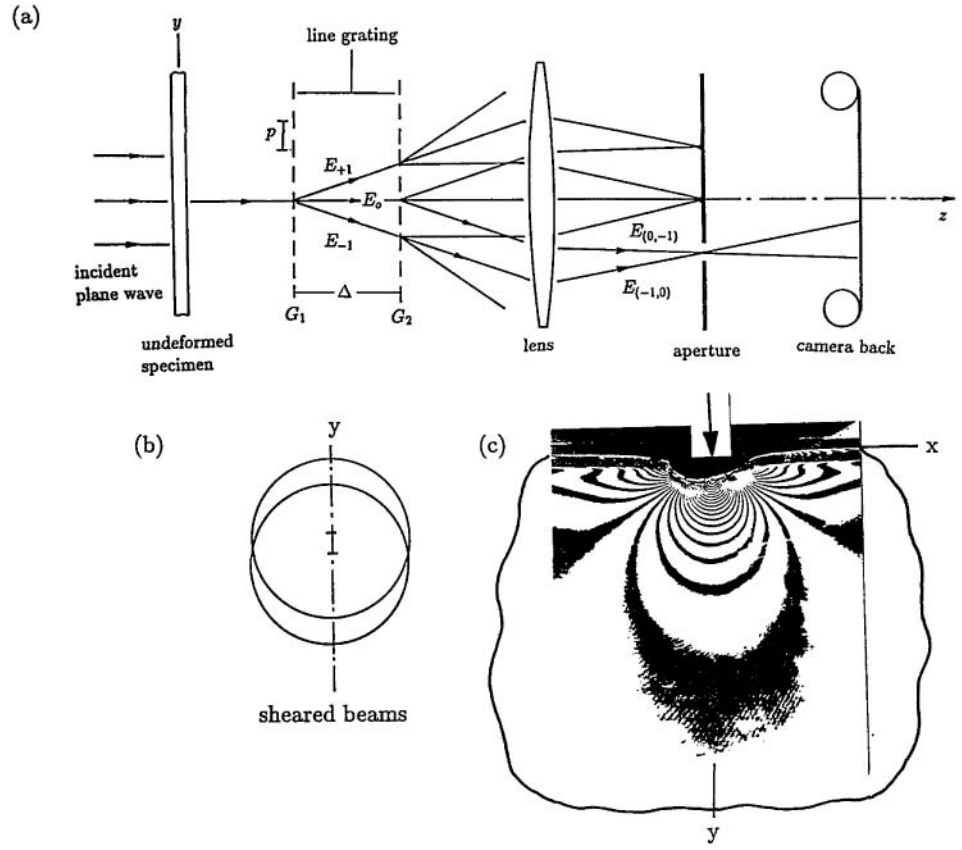


Fig. 1. (a) Optical arrangement and working principle for transmission CGS, (b) laterally sheared wave fronts on the camera back, (c) typical transmission CGS fringes for a line load acting on the edge of a half-space.

corresponding intensity distribution becomes

$$I = (E_0 + E_{-1})(E_0 + E_{-1})^* = (A^2 + B^2) + 2AB\cos[k(l_1 - l_2)], \quad (1)$$

where $A$ and $B$ are constants associated with $E_0$ and $E_{-1}$, respectively, $k$ is the wave number, $(\cdot)^*$ indicates a complex conjugate, and $l_1$ and $l_2$ are the optical paths of $E_0$ and $E_{-1}$, respectively, between the two gratings. The intensity represented by the above equation is maximum when $[k(l_1 - l_2)] = 2N\pi$, where $N = 0, \pm1, \pm2, \ldots$. Consider $(l_1 - l_2)$:

$$\begin{aligned}(l_1 - l_2) &= \Delta[1 - (\cos\theta)^{-1}] \\ &= \Delta[1 - (1 - \theta^2/2 + \cdots)^{-1}] \\ &\approx \Delta(\theta^2/2), \end{aligned} \quad (2)$$

where $\cos\theta$ is expanded in the neighborhood of zero and $O(\theta^3)$ is neglected when compared with $O(\theta^2)$ terms. Note, however, that a first-order approximation ($\cos\theta = 1$) would result in a zero optical path difference between $E_0$ and $E_{-1}$. From Eqs. (1) and (2) constructive interference occurs on the image plane when

$$\theta/2 = Np/\Delta, \quad (3)$$

wherein $k = 2\pi/\lambda$ and $\theta\lambda/p$ are used. Thus in ideal conditions for a uniform planar phase object the experimental parameters can be chosen to produce a uniformly bright fringe corresponding to the initial planarity of the object wave front.

Next consider a deformed specimen. The collimation of the incident light beam is perturbed by nonuniform changes in thickness and/or the refractive index of the specimen. Let the perturbed object wave front propagate in a direction so that it makes an angle $\phi$ with the optical axis [Fig. 2(b)]. Then the intensity distribution on the image plane is given by

$$I' = (A^2 + B^2) + 2AB\cos[k(l_1' - l_2')],$$

where

$$\begin{aligned}(l_1' - l_2') &= \Delta\{(\cos\phi)^{-1} - [\cos(\theta - \phi)]^{-1}\} \\ &= \Delta\{(1 - \phi^2/2 + \cdots)^{-1} \\ &\quad - [1 - (\theta - \phi)^2/2 + \cdots]^{-1}\} \\ &\approx \Delta(-\theta\phi + \theta^2/2). \end{aligned} \quad (4)$$

Again terms smaller than $\phi^2$, $\theta^2$, and $\phi\theta$ are neglected and $l_1'$, $l_2'$ are the optical path lengths of $E_0$ and $E_{-1}$ for the deformed specimen. The two quantities $\theta\phi$

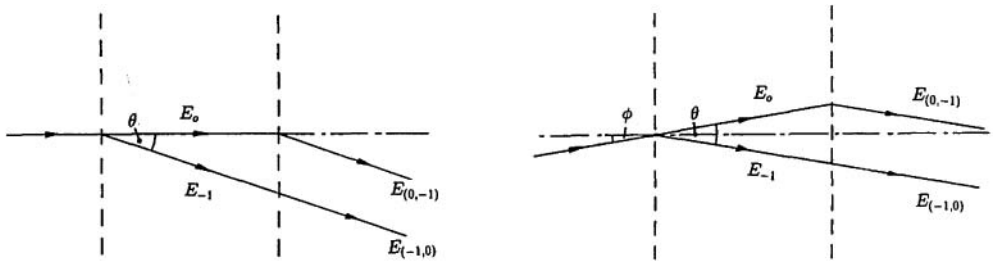


(a) (b)

Fig. 2. Wave-front shearing: (a) undeformed object wave front, (b) deformed object wave front.

and $\theta^2/2$ are of the same order, and the need for a second-order approximation for consistency throughout is obvious from Eqs. (2) and (4). Thus, for constructive interference,

$$k\theta(\theta/2 - \phi) = 2N'\pi, \quad N' = 0, \pm 1, \pm 2, \ldots,$$
$$(\theta/2 - \phi) = N'p/\Delta. \tag{5}$$

Note that in this case one could express the propagation vector $\mathbf{d}$ of the object wave front as $\mathbf{d} = \alpha\hat{e}_x + \beta\hat{e}_y + \gamma\hat{e}_z$, where $\alpha$, $\beta$, and $\gamma$ are the direction cosines and $\hat{e}_i$ are the unit normals in the $x$, $y$, and $z$ directions, respectively. For deflection of light rays shown in Fig. 2(b), $\alpha = 0$, $\beta = \sin\phi$, and $\gamma = \cos\phi$. For small angles, $\beta \approx \phi$. Hence, using Eq. (3), we can rewrite Eq. (5) as

$$\beta = \phi = (N - N')p/\Delta. \tag{6}$$

Thus CGS provides interference patterns that represent contours of constant $\beta$. Also, fringe order $N$ is independent of deformation and dependent only on the parameters $\lambda$, $\Delta$, and $p$ of the optical setup. Thus one can interpret Eq. (6) as simply

$$\beta = np/\Delta, \tag{7}$$

where $n = N' - N'$. In practice the optics are arranged so that initially a uniform bright field or a bright fringe is observed on the image plane when the object is undeformed. On deformation, $\beta$ changes locally from point to point resulting in interference patterns that represent deviations from the initial planarity of the wave front.

Note that the results [Eqs. (5)] obtained above are the same as those obtained through a Fourier optics analysis with the Fresnel approximation [see Eq. (18) in Ref. 4]. However, the result based on geometrical optics (Ref. 2) is slightly different; it suggests that $N = 0$ instead of $N =$ constant. An examination of Eq. (7) in Ref. 2 reveals the reason behind this minor difference between the two analyses; it is simply the order of approximation used in each case. A first-order analysis provides absolute fringe orders while the present analysis suggests that the fringe orders are relative with respect to the initial planarity of the object wave front. This analysis, however, would not affect the fringe interpretation when the test object is a homogeneous transparent planar object of constant thickness or a flat specularly reflective surface studied with a collimated beam of light. Furthermore, for completeness, the derivation in Ref. 2 can be easily recast in the form presented above. Consider the total amplitude distribution on the image plane obtained as given by Eq. (7) of Ref. 2:

$$(E_0 + E_{-1}) = A\exp\left(ik\frac{\Delta}{\gamma}\right) + B\exp\left(ik\frac{\Delta}{\gamma\cos\theta + \beta\sin\theta}\right), \tag{8}$$

where $\beta$ and $\gamma$ are the direction cosines of the propagation vector $\mathbf{d}$ of the object wave front as discussed above. For the beam of light shown in Fig. 2, $\alpha = 0$, $\beta = \sin\phi$, and $\gamma = \cos\phi$. By expressing $\beta$ and $\gamma$ in terms of $\phi$ in Eq. (8), we get

$$(E_0 + E_{-1}) = A\exp\left(ik\frac{\Delta}{\cos\phi}\right) + B\exp\left[ik\frac{\Delta}{\cos(\theta - \phi)}\right]. \tag{9}$$

Hence the intensity distribution becomes

$$I' = (A^2 + B^2) + 2AB\cos k\Delta\{(\cos\phi)^{-1} - [\cos(\theta - \phi)]^{-1}\}$$
$$= (A^2 + B^2) + 2AB\cos[k(l_1' - l_2')], \tag{10}$$

which provides the same result as Eq. (4).

Thus the resulting interference patterns observed in the CGS method are essentially contours of small angular deflections of light rays. They represent deviations from the initial planarity of the wave front. They can be further related to mechanical deformations as demonstrated in Refs. 2 and 4:

$$\beta = cB\frac{\partial(\sigma_x + \sigma_y)}{\partial y},$$
$$\alpha = cB\frac{\partial(\sigma_x + \sigma_y)}{\partial x}, \tag{11}$$

where $c$ is the elasto-optic constant for the phase object and $B$ is the nominal thickness of the specimen.

The author thanks the National Science Foundation Mechanics and Materials program for its support of the research through Research Initiation Award MSS-9109731.

## References

1. P. Hariharan, W. H. Steel, and J. C. Wyant, "Double grating interferometer with variable lateral shearing," Opt. Commun. **11,** 317 (1974).
2. H. V. Tippur, S. Krishnaswamy, and A. J. Rosakis, "Optical mapping of crack tip deformations using the methods of transmission and reflection coherent gradient sensing: a study of crack tip $K$-dominance," Int. J. Fracture **52,** 91–117 (1991).
3. H. V. Tippur and A. J. Rosakis, "Quasi-static and dynamic crack growth along bimaterial interfaces: a note on crack tip field measurements," Exp. Mech. **31,** 243–251 (1991).
4. H. V. Tippur, "Coherent gradient sensing: a Fourier optics analysis and applications to fracture," Appl. Opt. **31,** 4428–4439 (1992).
5. H. A. Bruck and A. J. Rosakis, "On the sensitivity of coherent gradient sensing: Part II—an experimental investigation of accuracy in fracture mechanics applications," Opt. Lasers Eng. **18,** 25–51 (1992).
6. H. V. Tippur and S. Ramaswamy, "Measurement of fracture parameters near cracks in homogeneous and bimaterial beams," Int. J Fracture **61,** 247–265 (1993).